UC Irvine
UC Irvine Previously Published Works

Title
Extended solubility of Sr in LaPO4 monazite

Permalink
https://escholarship.org/uc/item/98z3v7wv

Authors

Ohtaki, Kenta K
Heravi, Neshat J
Leadbetter, Joanne W
et al.

Publication Date
2016-10-01

DOI
10.1016/j.ssi.2016.05.022

Peer reviewed

Extended Solubility of Sr in LaPO$_4$ Monazite

Kenta K. Ohtaki, Neshat J. Heravi, Joanne W. Leadbetter, Peter E. D. Morgan, and Martha L. Mecartney*

Department of Chemical Engineering and Materials Science, University of

California, Irvine, CA, 92697, USA.

Corresponding author*: Martha L. Mecartney Tel: (949) 824-2919, Email address: martham@uci.edu

Abstract

Monazite-type LnPO$_4$ is a stable phase for many of the larger rare earths. The 9-fold coordinated La^{3+} sites can be substituted by other large ions including aliovalent ions such as Sr^{2+}. In the case of divalent ions, "charge balance" can be maintained by substituted monovalent anionic units such as (OH)$^-$. The solid solution series has the chemical formula La$_{1-x}$Sr$_x$PO$_{4-x}$(OH)$_x$, which can exist without apparent defects such as vacancies as long as sufficient water is present. X is demonstrated to be at least as high as 0.3 when using a direct precipitation process in hot, strong phosphoric acid. Physical properties of Sr-doped LaPO$_4$ up to that level, including proton transport, have been measured. At high temperature, (>400ºC) proton ionic conductivity in the bulk is expected to be high, but destabilization of the structure occurs. Sr leaves the structure and forms an intergranular phase with phosphorous, a process that detrimentally affects the ionic conductivity and cannot be suppressed even when conducting measurements in water vapor that should retain (OH)$^-$ in the structure.

Introduction

The hunt for good proton conducting oxides, such as perovskites and monazites,[1–5] has usually involved aliovalent cation doping which leads to vacancy and oxygen enhanced conducting pathways. It is understood to a degree how these protons interact with vacancies and oxygen anions.[6–8] In many minerals, aliovalent cation incorporation leads to substitution in the *anionic* lattice, including (OH)$^-$ replacing O^{2-}.[9] A particular case is the substitution of Sr^{2+} into LaPO$_4$ monazite. Theoretically, when Sr^{2+} is doped into LaPO$_4$ replacing La^{3+}, the structure can incorporate protons as (OH)$^-$ to compensate the effective charge difference between La^{3+} and Sr^{2+}. With x% of Sr replacing La, the stoichiometry will be La$_{1-x}$Sr$_x$PO$_{4-x}$(OH)$_x$. Protons are able to hop/tunnel from oxygen to oxygen providing a mechanism for ionic conductivity.[10] Therefore, divalent (Ca^{2+}, Sr^{2+})-doped LaPO$_4$ has been investigated as a prospective protonic conductive material.[11–13] Interestingly, the published research reports widely varying Sr substitutional concentrations [11,14–17] which may be due to different (OH)$^-$ content.

If (OH)$^-$ can be retained in the La$_{1-x}$Sr$_x$PO$_{4-x}$(OH)$_x$ monazite crystal structure, then high doping levels of Sr should produce high concentrations of protons and subsequently high ionic conductivity. At the limit of x=1, SrPO$_3$(OH) exists in three polymorphs, with γ-SrHPO$_4$ having Sr in 9-fold coordination similar to La in LaPO$_4$. [18] While it is tempting to think that a solid solution could exist from x = 0 to x = 1, the γ-SrHPO$_4$ crystal structure is orthorhombic while

LaPO$_4$ is monoclinic. Thus it cannot be expected that a continuous solid solution exists between SrPO$_3$(OH) and LaPO$_4$. This leaves the unresolved question as to the maximum possible solubility of Sr in La$_{1-x}$Sr$_x$PO$_{4-x}$(OH)$_x$ monazite that will generate a high protonic conductivity by maximizing the incorporation of (OH)$^-$.

Sr-doped LaPO$_4$ has been synthesized via several methods with widely varying maximum Sr concentrations: Microwave assisted hydrothermal processes (Sr$_{La}$ ~2%)[19], homogeneous precipitation in a controlled atmosphere (Sr$_{La}$ ~20%) [15], co-precipitation of La and Sr phosphates using (NH$_4$)$_2$HPO$_4$, La(NO$_3$)$_3$ and Sr(NO$_3$)$_2$ aqueous solutions (Sr$_{La}$ ~7%)[11], calcination where SrHPO$_4$ and LaPO$_4$ are mixed and calcined at 1000ºC (Sr$_{La}$ ~1%).[16] In many publications, the Sr content after sintering or calcination is not characterized. Many methods require a high temperature heat treatment (>700°C) to convert a Sr-doped rhabdophane (LaPO$_4$•½ H$_2$O) phase into monazite. Heat treatments in air lead to lower Sr concentrations in the LaPO$_4$ structure due to segregation of Sr and formation of a secondary phase.[17] The direct precipitation method used here [20], directly precipitates Sr-doped monoclinic LaPO$_4$ monazite without any heat treatment required. Theoretically via the direct precipitation method, Sr-doped LaPO$_4$ containing a high concentration of Sr can be synthesized.

Experimental

Synthesis

Sr-doped monoclinic LaPO$_4$ monazite was synthesized via the direct precipitation method.[20] La(NO$_3$)$_3$.6H$_2$O and Sr(NO$_3$)$_2$ are dissolved in DI water (using a minimum amount of water to dissolve nitrates) with certain molar ratio (Sr^{2+}:La^{3+}=10:90, 20:80, 30:70, 40:60, 50:50, 100:0) and dripped into H$_3$PO$_4$, which is pre-heated to 150 ºC to remove any residual water. The temperature of H$_3$PO$_4$ is kept at 150-160ºC while stirring. The Sr/La nitrate solution is added at a rate of 3 drops/min. As the nitrate solution is dripped into the H$_3$PO$_4$, the temperature of the solution is kept at 150-160 ºC to ensure all the water from the nitrate solution evaporates. Precipitation of white powders occurs after 4-5 hours. The obtained precipitate is washed with water until the pH reaches 7, then washed with ethanol and then acetone before drying the powder at 80 ºC.

Phase identification of the precipitate powders was conducted by X-ray diffraction (Rigaku SmartLab X-ray diffractometer). The unit cell volume of each powder is estimated by Rietveld refinement (PDXL). Morphology and particle size was observed by scanning electron microscope (FEI Magellan 400 XHR SEM). The Sr concentration of particles was measured by energy dispersive X-ray spectroscopy (EDS Oxford Instruments 80mm^2). For EDS, the powder samples were pressed into cylindrical pellets by cold isostatic pressing (55 kpsi). The Lα peak was used for La and Kα peak for Sr relative concentration determination by EDS. FTIR (Jasco FT/IR-4700 - ATR-PRO ONE) in a range of 400-4000cm^{-1} with 2cm^{-1} resolution was used to confirm that OH was retained in the structure of Sr-doped LaPO$_4$.

Evaluation of the stability as a function of temperature and effect of water vapor

To compare the high temperature stability of Sr-doped LaPO$_4$ powder as a function of Sr concentration (Sr$_{La}$ = 10, 20, 30%), powders were annealed in air at 800ºC for 10 h with 5ºC/min ramp rate. The 20% Sr$_{La}$ powders were also annealed in water vapor at 800ºC for 10 h. Pressed

powder pellets from the direct precipitation powders without any heat treatment (Sr_{La} = 10, 20, 30%) were sintered in water vapor at 1200ºC for 17 h with a ramp rate of 5ºC/min to retain $(OH)^{-}$ in the structure. To understand the effect of water vapor, 20% Sr_{La} pressed pellets were also sintered in air at 1200ºC for 17 h. The water vapor environment was created by bubbling compressed air through water heated in a bath at 60ºC, which generates 20% partial pressure of water vapor in the tube furnace. High temperature stability was evaluated by observing secondary phase formation and changes in unit cell volume by XRD.

Ionic conductivity

Impedance of Sr-doped $LaPO_4$ was measured by AC electrical impedance spectroscopy (EIS) (Hewlett Packard 4192A LF Impedance Analyzer) and converted into resistance by Z View (Scribner Associates). Resistance is converted into resistivity based on the sample geometry, and then changed to conductivity. A two probe method was used to measure the impedance.

The initial set of samples for EIS were cylinders 5-7mm diameter and 4-5mm thickness made by cold isostatic pressing and sintered at 1200 ºC in water vapor for 17 h. Pt coating with thickness of 60nm was sputtered on both surfaces in order to improve the contact between Pt plate electrodes and the sample with measurements from 300 to 650ºC. Pressed powder samples were also used for EIS from 300 to 650ºC *without* sintering (in order to avoid high temperatures) with Pt coating sputtered on both surfaces. Since the Pt coating degraded at high temperature, pressed powder samples *without* a Pt coating were also used in comparison for EIS measurements from 300 to1000ºC. The furnace temperature was held for an hour at each temperature and then the impedance was measured. EIS experiments were conducted in flowing water vapor or dry air as indicated.

Results

Synthesis

The XRD of $LaPO_4$ with different nominal Sr concentrations that correspond to the expected substitution of Sr for La (from the Sr/La ratios in the starting nitrate solutions) shows that to 40%, single phase $LaPO_4$ monazite is obtained (Fig. 1). At 50%, a trace of $Sr(H_2PO_4)_2$ forms as well as $LaPO_4$. When pure $Sr(NO_3)_2$ (Sr 100%) is mixed into the phosphoric acid, only $Sr(H_2PO_4)_2$ forms. Based on the XRD patterns, the unit cell volume was estimated by Rietveld refinement. Powders were washed with water before conducting XRD for Rietvelt refinement, but $Sr(H_2PO_4)_2$ dissolves in water, thus only $LaPO_4$ peaks were used for the refinement. As shown in Fig. 2, the unit cell volume of $LaPO_4$ increases with increasing nominal Sr concentration. The dashed line represents the linear trend generated by the first three data points, but above 30% the unit cell volume is lower than predicted by the trend line.
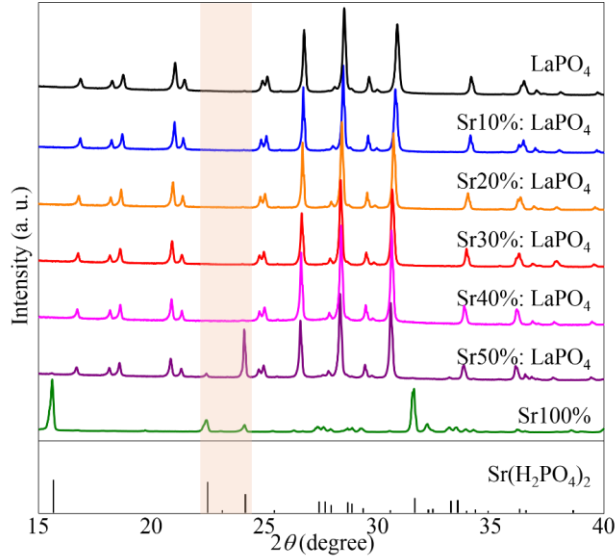
Fig. 1. XRD of Sr-doped LaPO$_4$ powders with nominal Sr$_{La}$ concentration of 10, 20, 30, 40, 50 and 100%. LaPO$_4$ peaks match the JCPDS data. [21] At 100% Sr$_{La}$, Sr(H$_2$PO$_4$)$_2$ is formed.[21] [22]
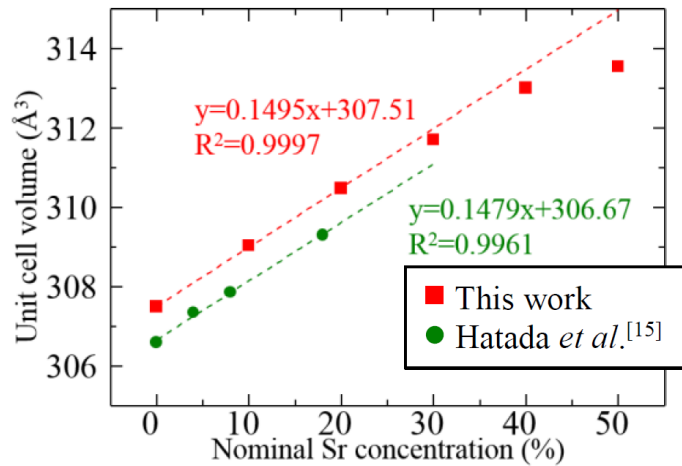

Fig. 2. Unit cell volume of monazite with different nominal Sr concentration (10-50%). The top dashed line (red) is generated by the first three data points. The green dashed line is generated from Hatada et al. [15] for concentrations of 0-20% Sr in monazite.

Fig. 3 shows SEM images prepared with different nominal Sr concentrations. The morphology and the particle size of Sr-doped LaPO$_4$ precipitates changes with increasing Sr concentration (Fig.3). 50% Sr$_{La}$ precipitates had to be washed only with ethanol and acetone so that the secondary phase (Sr(H$_2$PO$_4$)$_2$) remained (large dark crystals in a matrix of monazite seen in the pressed powder pellet in Fig. 3(g)). The same wash process had to be applied to retain the crystals for 100% Sr$_{La}$ (Fig. 3(h)).
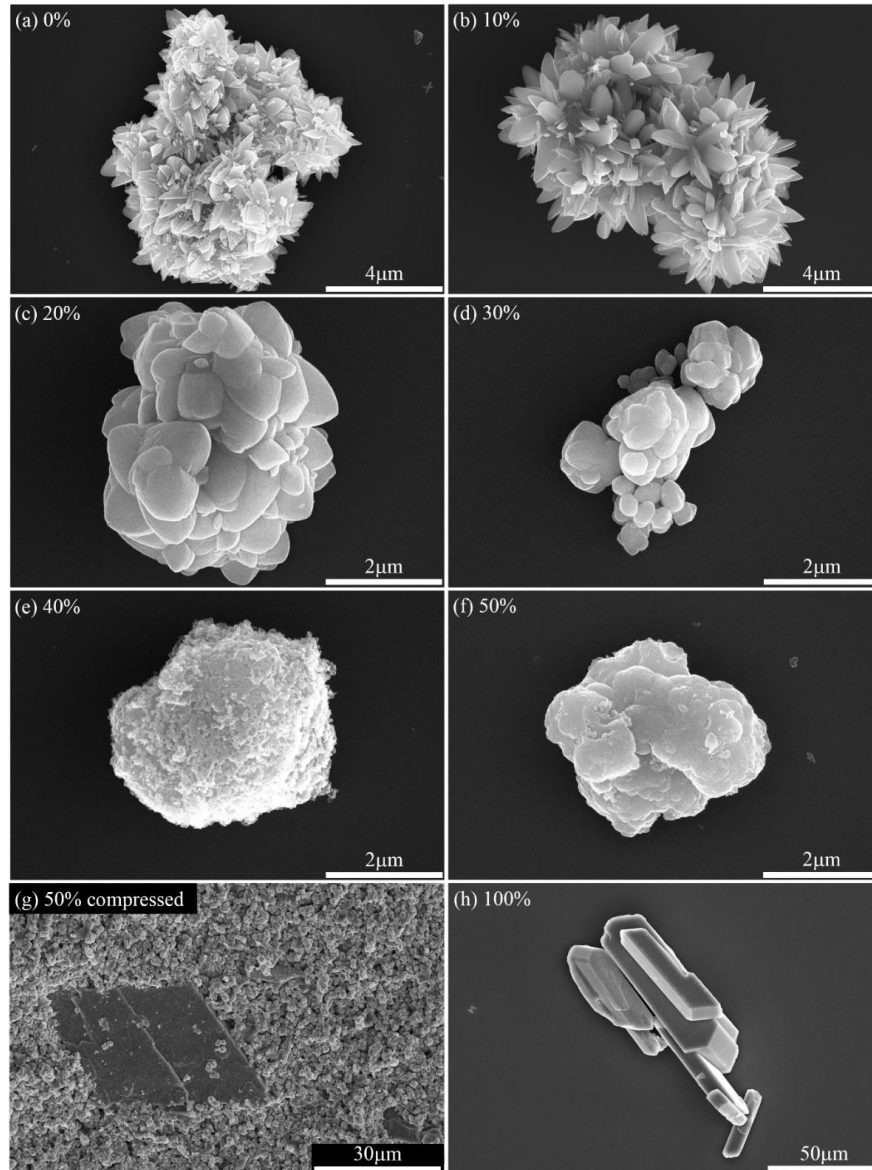
Fig. 3. SEM images of Sr-doped $LaPO_4$ powder precipitates with different nominal Sr_{La} concentrations. (a) 0%, (b) 10%, (c) 20%, (d) 30%, (e) 40%, (f) 50% (g) 50% pressed powder, (h) 100% Sr_{La} . The dark phase in (g) and the crystal in (h) are the Sr-rich phase ($Sr(H_2PO_4)_2$).

Table 1 shows the Sr_{La} concentration in pressed powder pellets as measured by EDS. The powders were washed with water, thus any $Sr(H_2PO_4)_2$ was washed away. At high nominal Sr_{La} concentration (>30%), the Sr concentration measured by EDS is lower than the expected concentration. The highest Sr concentration achieved is about 30% Sr_{La} in the 50% nominal concentration.

Table 1. Sr concentration measured by EDS

nominal Sr_{La} %	Sr/(Sr+La) measured by EDS (%)
10%	9.8 ± 0.33 (±3%)
20%	18 ± 0.27 (±2%)
30%	22 ± 0.51 (±2%)
40%	28 ± 0.31 (±1%)
50%	29 ± 0.35 (±1%)

Based on actual Sr concentrations measured by EDS, the unit cell volume of Sr-doped LaPO$_4$ is replotted in Fig. 4, and demonstrates a quasi-linear relationship with an R^2 value of 0.975.
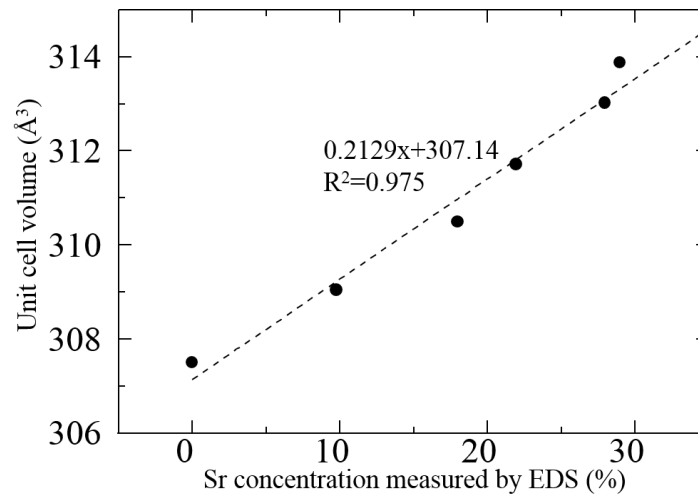

Fig. 4. Unit cell volume of monazite and "true" Sr_{La} concentration measured by EDS

The FTIR of Sr-doped LaPO$_4$ and LaPO$_4$ in Fig. 5 has an absorption at 875cm^{-1} that is assigned as the hydrogen-phosphate P-O-H stretching mode.[23] The peak intensity for this P-O-H increases with increasing Sr concentration.
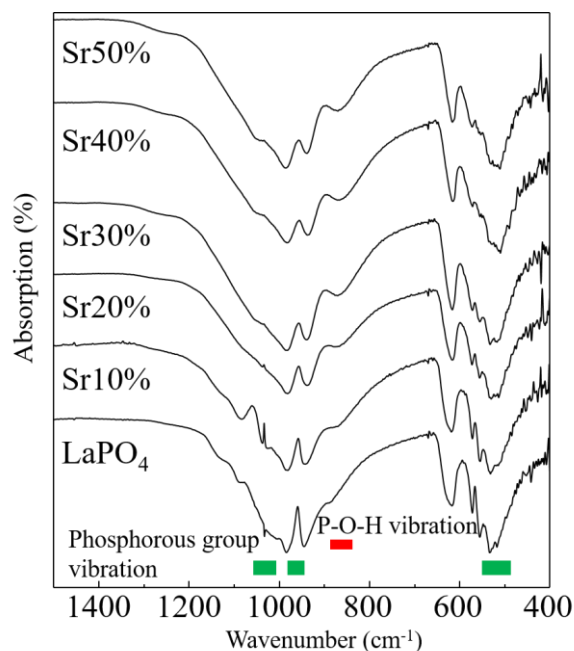
Fig. 5. FTIR of LaPO$_4$ and Sr-doped LaPO$_4$. The absorption around 875cm^{-1} is P-O-H vibrations (red band), absorption 542-615cm^{-1} are phosphate group v_4 vibrations, absorption at 960 cm^{-1} is phosphate group v_1 vibration and the absorption at 1015 cm^{-1} is phosphate group v_3 vibration (green bands). [24][25]

High temperature stability and effect of water vapor

In order to evaluate high temperature stability in air and in water vapor, Sr-doped LaPO$_4$ with different Sr concentrations was heat-treated. (The Sr concentration in the following graphs indicate the nominal concentration, not the true concentration by EDS.) XRD of Sr-doped LaPO$_4$ annealed in air at 800°C for 10 h shows Sr(PO$_3$)$_2$ forming after annealing (Fig. 6 (a)), while sintering in water vapor at 1200°C for 17 h forms Sr$_2$P$_2$O$_7$ (Fig. 6 (b)). The amount of the secondary phases increases with increasing initial Sr concentration.
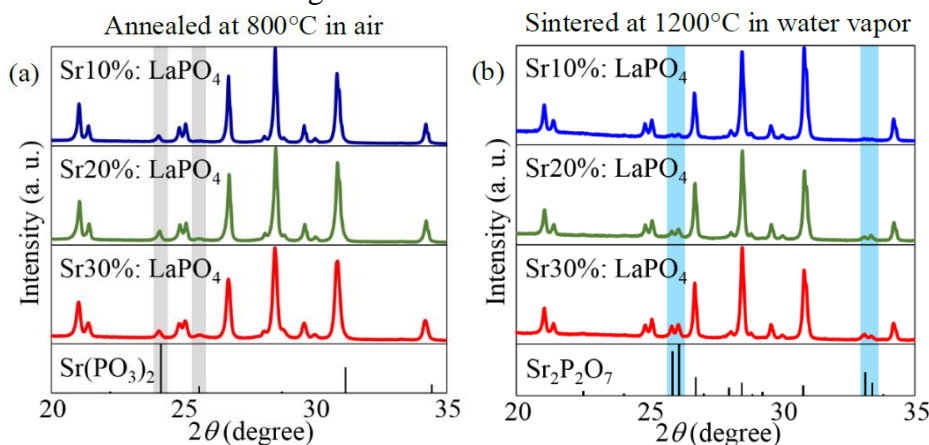
Fig. 6. (a) XRD of Sr10-30% LaPO$_4$ powder annealed at 800°C for 10 h in air. (b) XRD of Sr 10-30% doped LaPO$_4$ powder pellets sintered in water vapor at 1200°C for 17 h. Secondary phases that form from the monazite after annealing are indicated. All other peaks are LaPO$_4$.

The unit cell volume of Sr-doped LaPO$_4$ before and after each heat treatment are given in Fig. 7. The unit cell volume is reduced to that of pure LaPO$_4$ for both heat treatments. Even 100% LaPO$_4$ shows unit cell volume contraction after heat treatments. After sintering in water vapor, the Sr$_2$P$_2$O$_7$ formed is also clearly visible by SEM (Fig. 8).
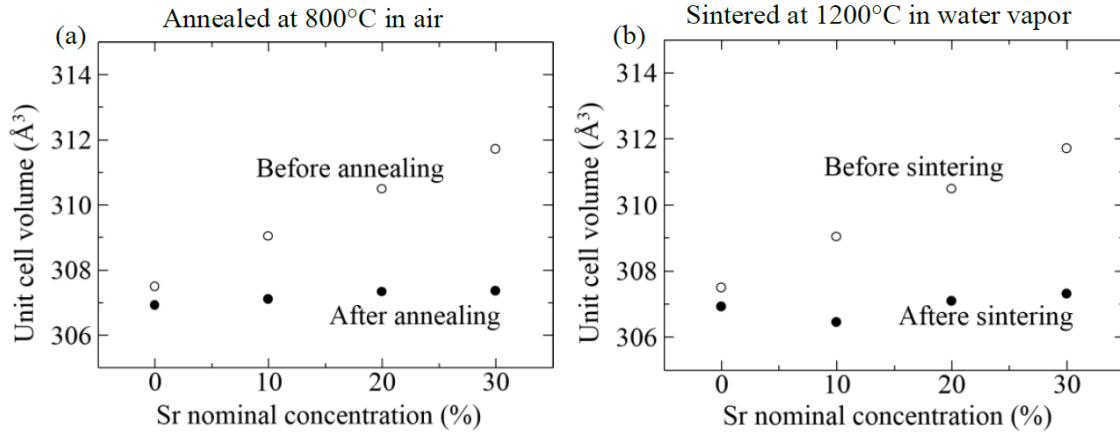

Fig. 7. (a) Unit cell volume before and after annealing at 800°C for 10 h in air. (a) Unit cell volume before and after sintering at 1200°C for 17 h in water vapor.
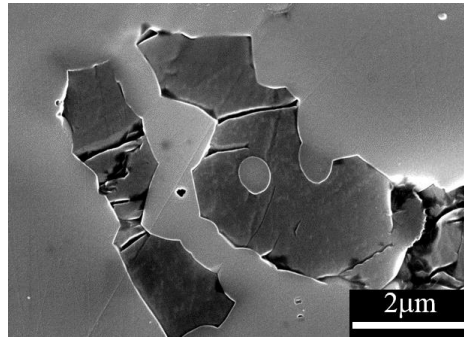
○: before heat treatment, ●: after heat treatment

Fig. 8. Secondary electron SEM image of Sr$_{La}$ 30% doped LaPO$_4$ sintered at 1200°C in water vapor. The dark phase is the Sr-rich Sr$_2$P$_2$O$_7$. Light phase is LaPO$_4$.

One composition (20% Sr$_{La}$) was selected to compare the effect of heating with water vapor or dry air (Fig. 9). At 1200°C both in air and in water vapor, Sr$_2$P$_2$O$_7$ formed. In contrast, at 800°C large amounts of Sr(PO$_3$)$_2$ were produced by annealing in air whereas no secondary phases are detectable after annealing in water vapor.
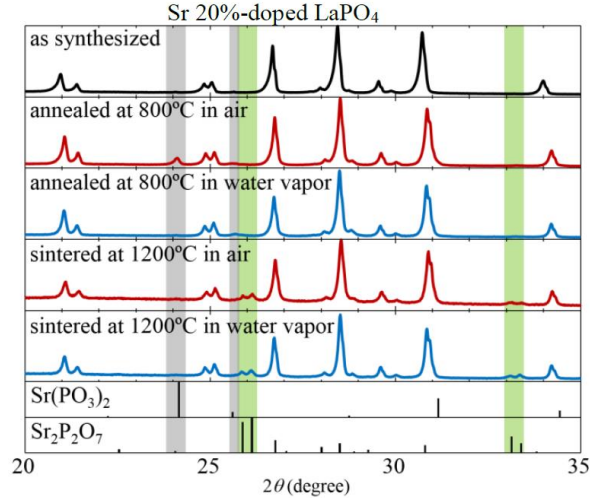
Fig. 9. XRD of Sr 20% doped LaPO$_4$ after heat treatment in air and in water vapor.

Ionic conductivity

The ionic conductivity measured in water vapor at 300-600°C for samples sintered in water vapor and pressed powder pellets and compared with results from Amezawa et al. [12] in Fig. 10. Around 550°C, conductivity drops for the sintered samples and the Pt coating was found to be degraded after the measurement. The density of each sintered sample was low (~60%). Pressed powder pellets with a density of ~55% without sintering showed an order of magnitude *higher* conductivity than sintered samples, despite a similar low density. However, ionic conductivity also dropped significantly for the pressed pellets around 500°C due to degradation of the Pt coating. No secondary phase was detected after EIS by XRD, but any amorphous phases would not be detectable.
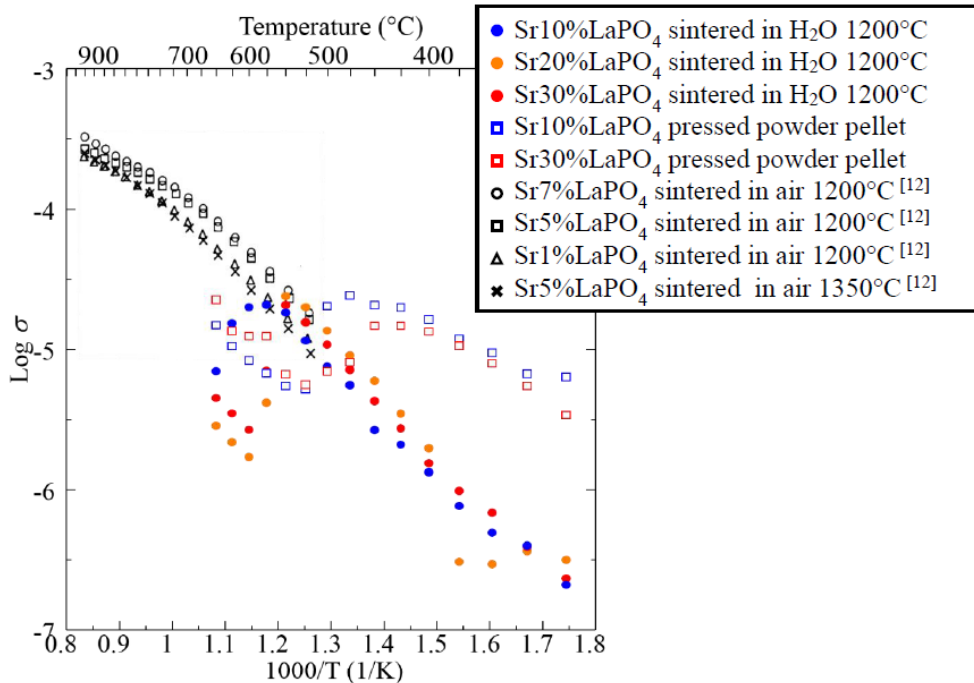
Fig. 10. EIS measurement of ionic conductivity in water vapor for sintered powder and pressed powder pellets with Pt coating (300°C-650°C).

EIS measurements in water vapor of pressed powder pellets without a Pt coating (Fig. 11) show lower initial conductivity than those with a Pt coating (Fig. 10) as expected due to poorer contact with Pt electrode plates, but the conductivity did not drop at as temperature increased, supporting the observation that the Pt coating degrades at high temperatures.
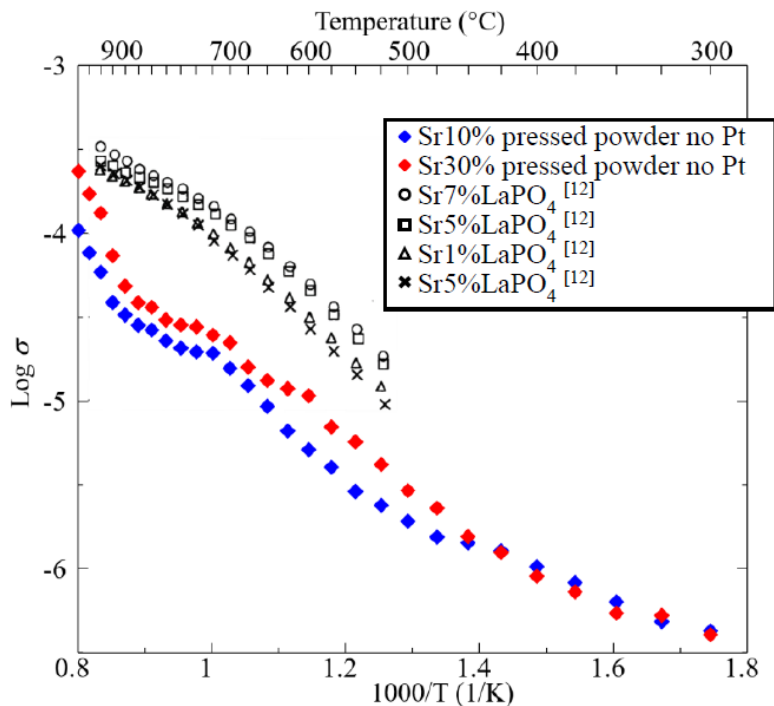
Fig. 11. Conductivity measured in water vapor for pressed powder pellets without Pt coating

After EIS measurements in water vapor to 1000°C of pressed powder pellets without Pt coatings, XRD found no secondary phases for 10% Sr_{La} but for 30% Sr_{La} the phase $Sr_2P_2O_7$ had formed, the same as for 20% Sr_{La} (Fig. 9). For 30% Sr_{La}, the P-O-H vibration disappeared and P-O-P vibration appeared in the FTIR spectra (Fig. 12).
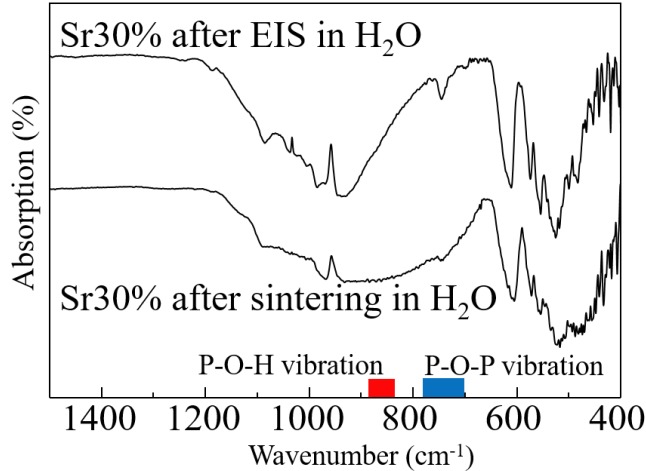
Fig. 12. FTIR of Sr-doped LaPO$_4$ pressed powder pellets after EIS measurement and after sintering in water vapor. The absorption around 875cm^{-1} is the P-O-H vibration and the absorption around 750 cm^{-1} is the P-O-P vibration, which is due to Sr$_2$P$_2$O$_7$ formation.

Discussion

Synthesis

The calculated ionic radius of Sr^{2+} is 1.31 Å and that of La^{3+} is 1.22 Å in 9-fold coordination.[26] Thus the volume expansion in Fig. 2 is due to Sr^{2+} replacing La^{3+} in the LaPO$_4$ structure. This volume expansion with increasing Sr concentration was also reported by Hatada *et al.*[15] As the nominal Sr concentration reaches the solubility limit in LaPO$_4$ made via the direct precipitation method, it becomes more difficult to incorporate further Sr into the LaPO$_4$ structure (Fig. 4). Based on XRD and EDS results, the solubility limit of Sr in LaPO$_4$ is around 30% for the precipitation temperature used (150-160°C). After heat treatments, the unit cell volume of pure LaPO$_4$ decreased (Fig. 7), which implies that LaPO$_4$ synthesized via this method is not at equilibrium as synthesized. This might explain why the initial unit cell differs the unit cell volume reported by others, and why the lattice parameters of LaPO$_4$ monazite are smaller when synthesized at higher temperatures [15,21] We do not discount the possibility that there may be a higher Sr concentration reachable in LaPO$_4$ using different method. Our method with so much excess phosphoric acid might lead via the natural chemistry of Sr to the formation of Sr(H$_2$PO$_4$)$_2$, limiting this method to a Sr$_{La}$ concentration of 30%. As the concentration of Sr^{2+} ions in the reactant solution increases, the morphology of the precipitates becomes rounded (Fig. 3), indicating a lower surface energy anisotropy than for pure LaPO$_4$.

As shown in the FTIR spectra (Fig. 5), the strong absorption for P-O-H bonding is observed around 875 cm^{-1} for the precipitated powders and increases with Sr concentration. This indicates that (OH)$^-$ is incorporated and bonded to phosphorous atoms in the LaPO$_4$ structure as Sr^{2+} replaces La^{3+} in the structure. However, the P-O-H bonding absorption in nominal 40% and 50% Sr$_{La}$ are almost the same. This correlates with the EDS (Table 1) and XRD results (unit cell volume expansion) that imply that the solubility limit of Sr using the direct precipitation method is around 30%, since both of these nominal compositions of 40% and 50% Sr$_{La}$ had only around 30% Sr$_{La}$ in the structure. This high concentration of Sr$_{La}$ is only possible by the incorporation of protons

from the H_3PO_4 solution. Heating the phosphoric acid to a high temperature to remove water from the system (150-160°C) is the key to preventing the formation of rhabdophane. Having an easily incorporated source of protons from the phosphoric acid is key to the high concentration of Sr^{2+} that can replace La^{3+} with $(OH)^-$ replacing O^{2-}.

High temperature stability and effect of water vapor

In this work, care was taken to compare samples that were heated only in water vapor and never dried, with samples that were exposed to air at high temperatures, where it can be presumed the protons are lost to the air as H_2O. In air, after high temperature heat treatments both Sr-rich phosphate secondary phases and contraction of the $LaPO_4$ unit cell volume were observed. There are many reports in the literature claiming that they obtained single phase monazite with doped Sr after high temperature heat treatments in air. [13,15] However, according to Fig. 6, $Sr(PO_3)_2$ should form at 800°C in air, the temperature which is conventionally used to convert rhabdophane to monazite. After sintering at higher temperature, reports mostly show by XRD single phase $LaPO_4$, perhaps because for low Sr concentrations (<5% Sr), the amount of secondary phase is below the XRD detection limit.

Segregation of Sr, formation of a secondary phase and volatilization of H_2O at high temperature have been reported by Tyholdt et al.[17] and Hatada et al.[15] Hatada et al. reported that after heating Sr-doped $LaPO_4$ at 800°C in N_2 environment, H_2O evaporated and the unit cell volume decreased and $Sr_2P_2O_7$ formed after sintering at 1200°C for 5 hours. Since the P-O-H vibration peak in FTIR disappears (Fig. 12) and $Sr_2P_2O_7$ forms after sintering, segregation of Sr must be induced by volatilization of H_2O at high temperature (1200°C) in our study too. The reaction of losing OH and formation of $Sr_2P_2O_7$ can be described as follows.

$$2Sr(OH)PO_3 \rightarrow Sr_2P_2O_7 + H_2O$$
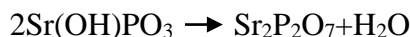
Introducing water vapor into the system in these current experiments was supposed to suppress volatilization of H_2O (OH in Sr-doped $LaPO_4$) and keep Sr in the $LaPO_4$ structure. Water vapor did help suppress formation of $Sr(PO_3)_2$ at 800°C. However, after annealing 20% Sr in water vapor at 800°C, the unit cell volume decreased from 310 $Å^3$ to 307 $Å^3$ (same value as pure $LaPO_4$ after annealing) indicating loss of Sr from the structure despite the fact that no Sr-rich phase crystallized in significant amounts (Fig. 9). Formation of $Sr(PO_3)_2$ from Sr-doped powders annealed in air at 800°C requires excess phosphorous since the ratio of Sr and P is 1:2. The excess phosphorous may be a result of residual phosphoric acid from the synthesis process, even though the powders are washed and milled with ammonia to remove the phosphorous on the surface of particles. At 1200°C in water vapor and in air, Sr-doped $LaPO_4$ forms a different secondary Sr-rich phase, $Sr_2P_2O_7$. Thus Sr-doped $LaPO_4$ is not stable at high temperature even in water vapor (at least with 20% partial pressure of water vapor). It should be noted that although water vapor suppresses formation of secondary phases at 800°C, there is still the contraction of the unit cell volume indicating loss of Sr. Under a water vapor environment at low temperature (~800°C), Sr-rich amorphous phases might be more favorable than Sr-rich crystalline phases.

Ionic conductivity measurements

The ionic conductivity for the samples sintered and tested in water vapor (Sr: 10 - 30%) at 300-600°C is similar to the conductivity reported by Amezawa et al. [12] (Fig. 10). They sintered samples in air, before testing by EIS in water vapor, so it is not surprising that the results overlap since Sr is lost during sintering at these high temperatures, whether in air or in water vapor. Their materials had nominal Sr_{La} concentrations of 1-7% as measured by ICP before sintering. After sintering at 1200°C and 1350°C in air, they did not report any data on the Sr_{La} concentration in the monazite grains.

Our Sr-doped monazite at 1200°C forms $Sr_2P_2O_7$ and the resultant Sr_{La} concentration in the $LaPO_4$ crystal structure is almost zero based on unit cell volume comparisons (Fig.7). The disappearance of the P-O-H vibration in the FTIR spectra (Fig. 12) is another suggestion of loss of Sr that would correlate with loss of OH^- during EIS measurements at high temperatures and after sintering in water vapor at 1200°C. Likewise the appearance of the P-O-P vibration, which is not present in monazite, correlates with the formation of $Sr_2P_2O_7$. With the loss of $(OH)^-$ in the structure as confirmed by FTIR (Fig. 12), it is not surprising that the conductivity of the high Sr_{La} concentrations in the low temperature range of 300-450°C is not higher than the data reported by Amezawa *et al.*[12] for Sr-doped $LaPO_4$ samples (Fig. 10). Sr-doped $LaPO_4$ has higher conductivity when the powder is pressed into pellets and not sintered nor exposed to high temperatures (Fig. 10). The bad news is that sintering is required to obtain dense ceramics useful as electrolytes, but sintering causes the formation of the secondary phase $Sr_2P_2O_7$ and loss of OH in the structure which decreases the conductivity.

Measurements of conductivity of pressed powder pellets of Sr-doped (10% and 30%) $LaPO_4$ without Pt coatings exhibit a kink at 700°C when the Sr-rich phosphate phases are expected to form, but then the conductivity starts increasing again up to 1000°C. Sr-doped $LaPO_4$ has p-type electronic conductivity that dominates once high temperatures have been reached (600-800°C).[13] Assuming that Sr-doped $LaPO_4$ does not contain mobile protons after being exposed to air at high temperatures and losing $(OH)^-$ and Sr_{La}, the increase in conductivity after 700°C must be due to the native electronic conductivity.

Although the sputtered Pt coatings degraded around 550°C for Sr-doped $LaPO_4$, the Pt coating do improve the connection between the sample and the electrode plates. Comparing Fig. 10 and Fig. 11 the conductivity is ten times higher using a Pt coating. Moreover, the pressed powder samples have ~45% porosity (55% dense). In order to roughly approximate the conductivity that could be expected without porosity, Bruggeman's model [27] was used. The conductivity of pores is assumed to be zero, and for this model only two phases are considered; porosity and Sr-doped $LaPO_4$. In the equation below, σ^* is predicted conductivity without porosity, σ_{eff} is the effective conductivity that was measured and V_{pore} is the volume fraction of porosity.

$$\sigma^* = \frac{\sigma_{eff}}{1 - 1.5 V_{pore}}$$

Since relative density of samples is around 55%, and the predicted conductivity is $3.1 \times \sigma_{eff}$. The model assumes porosity is below the percolation limit, so this result can be considered a lower limit for the predicted conductivity.

If the correction for porosity is combined with the calculation of increased conductivity if the samples are coated with Pt that does not degrade at high temperature, the conductivity of these materials with Sr-doped $LaPO_4$ may be as high as shown theoretically in Fig. 13. This theoretical conductivity is higher than previously reported ionic conductivity for Sr doped $LaPO_4$, however, the conductivity is still too low for practical application as a proton conducting electrolyte due to the formation of Sr-rich phases, depleting the Sr_{La} and causing a loss of $(OH)^-$. Despite the expectation that Sr-doping in $LaPO_4$ should generate highly mobile protons as predicted by theory, [8,10] the inability to retain Sr_{La} in the monazite crystal structure at high temperatures precludes the realization of this promise.
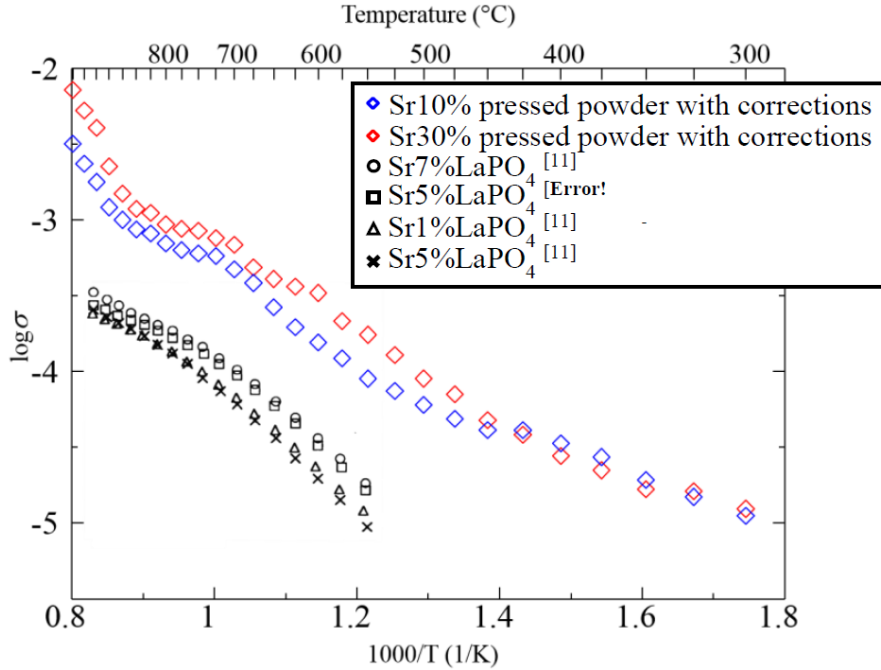

Fig. 13. Theoretical conductivity in water vapor of Sr-doped $LaPO_4$ with porosity correction and if intact Pt coating was used.

Conclusions

Highly doped Sr-doped $LaPO_4$ was successfully synthesized via the direct precipitation method. Using this method, the solubility limit of Sr^{2+} replacing La^{3+} in monoclinic $LaPO_4$ powders is approximately 30%, which is the highest Sr_{La} concentration reported to date for monazite. Increasing Sr_{La} concentration could be correlated with increased $(OH)^-$ replacing O^{2-}. Although there is not a complete solid solubility from $LaPO_4$ to $SrPO_3(OH)$, this study shows possible directions for further research on other hydroxide containing oxides that could be potentially new proton conductors.

However, as temperature increases, $(OH)^-$ is lost and Sr^{2+} leaves the structure forming Sr-phosphate secondary phases. While a partial pressure of 20% water vapor prevents the formation of crystalline Sr-phosphate phases at intermediate temperatures, it is not sufficient to retain $(OH)^-$ and Sr_{La} in the structure at temperatures required for sintering (>1200°C). Thus, for all practical purposes, with the depletion of Sr_{La}, the ionic conductivity is lower than desired so it will be

difficult to use these highly Sr-doped $LaPO_4$ powders as a conventional proton conductor. This does not preclude uses for other application where highly doped Sr monazite powders are preferred over sintered compacts, and where the material does not need to be exposed to higher temperatures.

References

1. Minh, N. G. Ceramic Fuel Cells. *J. Am. Ceram. Soc.* **76,** 563–588 (1993).

2. Kreuer, K.-D. Proton conductivity: materials and applications. *Chem. Mater.* **8,** 610–641 (1996).

3. Kreuer, K.-D., Paddison, S. J., Spohr, E. and Schuster, M. Transport in Proton Conductors for Fuel-Cell Applications: Simulations, Elementary Reactions, and Phenomenology. *Chem. Rev.* **104,** 4637–4678 (2004).

4. Kreuer, K. D. Proton conducting Oxides. *Annu. Rev. Mater. Res.* **33,** 333–359 (2003).

5. Kreuer, K. D. Aspects of the formation and mobility of protonic charge carriers and the stability of perovskite-type oxides. *Solid State Ion.* **125,** 285–302 (1999).

6. Bonanos, N., Huijser, A. and Poulsen, F. W. H/D isotope effects in high temperature proton conductors. *Solid State Ion.* **275,** 9–13 (2015).

7. Phadke, S., Nino, J. C. and Islam, M. S. Structural and defect properties of the $LaPO_4$ and LaP5O14-based proton conductors. *J. Mater. Chem.* **22,** 25388 (2012).

8. Yu, R. and DeJonghe, L. C. Proton-Transfer Mechanism in $LaPO_4$. *J. Phys. Chem. C* **111,** 11003–11007 (2007).

9. Rossman, G. R. Studies of OH in nominally anhydrous minerals. *Phys. Chem. Miner.* **23,** 299–304 (1996).

10. Toyoura, K. Hatada, N., Nose Y., Tanaka I., Matsunaga K. and Uda T.. Proton-Conducting Network in Lanthanum Orthophosphate. *J. Phys. Chem. C* **116,** 19117–19124 (2012).

11. Norby, T. and Niels Christiansen. Proton conduction in Ca-and Sr- substituted LaPO$_4$. *Solid State Ion.* **77,** 240–243 (1995).

12. Amezawa, K., Maekawa, H., Tomii, Y. and Yamamoto, N. Protonic conduction and defect structures in Sr-doped LaPO$_4$. *Solid State Ion.* **145,** 233–240 (2001).

13. Amezawa, K., Kjelstrup, S., Norby, T. and Ito, Y. Protonic and Native Conduction in Sr-Substituted LaPO$_4$ Studied by Thermoelectric Power Measurements. *J. Electrochem. Soc.* **145,** 3313–3319 (1998).

14. Glorieux, B., Montel, J. M. and Matecki, M. Synthesis and sintering of a monazite–brabantite solid solution ceramics using metaphosphate. *J. Eur. Ceram. Soc.* **29,** 1679–1686 (2009).

15. Hatada, N., Nose, Y., Kuramitsu, A. and Uda, T. Precipitation behavior of highly Sr-doped LaPO4 in phosphoric acid solutions. *J. Mater. Chem.* **21,** 8781 (2011).

16. Kitamura, N. Amezawa K, Tomii I., Hanada T., Yamamoto N., Omata T. and Otsuka S. Electrical Conduction Properties of Sr-Doped LaPO$_4$ and CePO$_4$ under Oxidizing and Reducing Conditions. *J. Electrochem. Soc.* **152,** A658 (2005).

17. Tyholdt, F., Horst, J. A., Jorgensen, S., Ostvold, T. and Norby, T. Segregation of Sr in Sr-doped LaPO$_4$ ceramics. *Surf. Interface Anal.* **30,** 95–97 (2000).

18. Ben Taher L., Smiri, L., Laligant, Y. and Maisonneuve, V. Investigation of the Alkaline Earth Phosphates: Synthesis and Crystal Structure of a New Strontium Hydrogen Phosphate Form. *J. Solid State Chem.* **152,** 428–434 (2000).

19. Colomer, M. T., Delgado, I., Ortiz, A. L. and Fariñas, J. C. Microwave-assisted Hydrothermal Synthesis of Single-crystal Nanorods of Rhabdophane-type Sr-doped LaPO$_4$ ·nH$_2$O. *J. Am. Ceram. Soc.* **97,** 750–758 (2014).

20. Schatzmann, M. T., Mecartney, M. L. and Morgan, P. E. D. Synthesis of monoclinic monazite, LaPO4, by direct precipitation. *J. Mater. Chem.* **19,** 5720 (2009).

21. Ni, Y., Hughes, J. M. and Mariano, A. N. $LaPO_4$ PDF card: JCPDS 01-083-0651. *Am. Mineral.* **80,** 21 (1995).

22. Frazier, A. W. Thrasher R. D., Weastad K. R., Hunter S. R., Kohler J. J. and Scheib M. $Sr(H_2PO_4)_2$ PDF card: JCPDS 00-044-0797. *Crystallogr Prop Fertil. Cmpds Bull* **y-217II,** (1991).

23. Lucas, S., Champion, E., Bregiroux, D., Bernache-Assollant, D. and Audubert, F. Rare earth phosphate powders $RePO_4 \cdot nH_2O$ (Re=La, Ce or Y)—Part I. Synthesis and characterization. *J. Solid State Chem.* **177,** 1302–1311 (2004).

24. Han, J., Wang, L. and Wong, S. S. Morphology and dopant-dependent optical characteristics of novel composite 1D and 3D-based heterostructures of CdSe nanocrystals and $LaPO_4$:Re (Re = Eu, Ce, Tb) metal phosphate nanowires. *RSC Adv.* **4,** 34963 (2014).

25. Ahsan, M. R. and Mortuza, M. G. Infrared spectra of $xCaO(1-x-z)SiO_2zP_2O_5$ glasses. *J. Non-Cryst. Solids* **351,** 2333–2340 (2005).

26. Shannon R. D. Revised Effective Ionic Radii and Systematic Studies of Interatoimic Distances in Halides and Chalcogenides. *Acta Cryst* **A32,** 751–767 (1976).

27. Bruggman, D. A. G. Calculation of various physics constants in heterogenous substances I Dielectricity constants and conductivity of mixed bodies from isotropic substances. *Ann Phys* **24,** 636–64 (1935).